nature biotechnology

ARTICLES

Enhancing T cell therapy through TCR-signaling-responsive nanoparticle drug delivery

Li Tang[1–3,11,12], Yiran Zheng[1,3,12], Mariane Bandeira Melo[1,3], Llian Mabardi[1], Ana P Castaño[4], Yu-Qing Xie[5], Na Li[1,3], Sagar B Kudchodkar[6], Hing C Wong[7], Emily K Jeng[7], Marcela V Maus[4,8] & Darrell J Irvine[1–3,9,10]

Adoptive cell therapy (ACT) with antigen-specific T cells has shown remarkable clinical success; however, approaches to safely and effectively augment T cell function, especially in solid tumors, remain of great interest. Here we describe a strategy to 'backpack' large quantities of supporting protein drugs on T cells by using protein nanogels (NGs) that selectively release these cargos in response to T cell receptor activation. We designed cell surface–conjugated NGs that responded to an increase in T cell surface reduction potential after antigen recognition and limited drug release to sites of antigen encounter, such as the tumor microenvironment. By using NGs that carried an interleukin-15 super-agonist complex, we demonstrated that, relative to systemic administration of free cytokines, NG delivery selectively expanded T cells 16-fold in tumors and allowed at least eightfold higher doses of cytokine to be administered without toxicity. The improved therapeutic window enabled substantially increased tumor clearance by mouse T cell and human chimeric antigen receptor (CAR)-T cell therapy *in vivo*.

Adoptive transfer of tumor-specific T cells has been shown to elicit tumor regression in patients with leukemia or melanoma, with some patients experiencing durable complete responses[1–3]. Adjuvant treatments that are aimed at increasing the fraction of responders and extending ACT to other solid tumors are thus under intensive study[4]. The administration of supporting cytokines (such as interleukins) or tumor-microenvironment-modulating factors are two central approaches that have been explored in preclinical and clinical studies to enhance T cell therapy[5,6]. However, supplying adjuvant drugs at the right time and site appears crucial, as systemically administered immunomodulators can have toxic effects[7,8]. Genetic engineering of T cells to express adjuvant cytokines in response to T cell receptor (TCR)-regulated transcription factors has been pursued in an attempt to focus cytokine delivery in the tumor microenvironment, but these approaches to date have still shown substantial toxicity in patients, which is thought to be due, in part, to wide variation in T cell gene expression among individuals[9].

In previous work, we described a complementary chemistry-based approach to delivering adjuvant drugs during adoptive therapy via conjugation of drug-loaded lipid nanoparticles (which we referred to as 'backpacks') to the plasma membrane of ACT T cells[10–12]. Nanoparticles that were covalently coupled to cell surface proteins were not internalized, and they allowed for potent autocrine stimulation of transferred T cells, leading to enhanced T cell persistence and function *in vivo*[11]. However, two important limitations of this approach were (i) the low drug-loading capacity achievable with traditional encapsulation strategies for protein drugs in nanoparticles and (ii) the lack of regulation of drug release, which was mediated by spontaneous slow leakage of drug cargos from the nanoparticle backpacks.

Here we demonstrate an approach to address these challenges and describe a strategy that chemically links adjuvant drug delivery to T cell activation by using TCR-signaling-responsive nanoparticle backpacks. Using a human interleukin (IL)-15 super-agonist (IL-15Sa) as a testbed drug cargo, we found that T cells backpacked with TCR-responsive NGs expanded 16-fold more in tumors than T cells supported by systemic cytokine injections, while remaining largely quiescent in the peripheral blood. This regulated drug release allowed eightfold more IL-15Sa to be administered safely in mice as compared to that with the free cytokine, enabling substantially improved therapeutic efficacy.

RESULTS

Design of protein nanogels responsive to changes in cell surface redox activity

Mammalian cells actively perform oxidation and reduction reactions in the face of the extracellular oxidizing environment through a family of transmembrane oxidoreductase enzymes[13]. Motivated by the fact that activated T cells have elevated levels of cell-surface

[1]David H. Koch Institute for Integrative Cancer Research, Massachusetts Institute of Technology (MIT), Cambridge, Massachusetts, USA. [2]Department of Materials Science and Engineering, Massachusetts Institute of Technology, Cambridge, Massachusetts, USA. [3]Department of Biological Engineering, Massachusetts Institute of Technology, Cambridge, Massachusetts, USA. [4]Cellular Immunotherapy Program, Massachusetts General Hospital (MGH) Cancer Center, Charlestown, Massachusetts, USA. [5]Institute of Bioengineering, École Polytechnique Fédérale de Lausanne, Lausanne, Switzerland. [6]Vaccine Center, Wistar Institute, Philadelphia, Pennsylvania, USA. [7]Altor BioScience Corporation, Miramar, Florida, USA. [8]Harvard Medical School, Boston, Massachusetts, USA. [9]Ragon Institute of Massachusetts General Hospital, Massachusetts Institute of Technology, Cambridge, Massachusetts, USA. [10]Howard Hughes Medical Institute, Chevy Chase, Maryland, USA. [11]Present addresses: Institute of Bioengineering, École Polytechnique Fédérale de Lausanne, Lausanne, Switzerland; Institute of Materials Science and Engineering, École Polytechnique Fédérale de Lausanne, Lausanne, Switzerland. [12]These authors contributed equally to this work. Correspondence should be addressed to L.T. (li.tang@epfl.ch) or D.J.I. (djirvine@mit.edu).

Received 4 June 2016; accepted 7 June 2018; published online 9 July 2018; doi:10.1038/nbt.4181

free thiols relative to those in naive cells (**Supplementary Fig. 1a**)[14], we measured the cell surface reduction activity of naive or activated T cells by using WST-1, a membrane-impermeable compound that forms a colored product following reduction[15,16]. Primed CD8$^+$ T cells showed higher cell surface reduction rates than naive T cells (**Fig. 1a**). However, T cell surface redox activity further increased following stimulation with antigen-presenting cells or with anti-CD3– and anti-CD28–coated beads (hereafter referred to as 'anti-CD3/CD28 beads') (**Fig. 1a**,**b** and **Supplementary Fig. 1b**).

We reasoned that increased redox activity at the T cell surface could be exploited to obtain antigen-triggered adjuvant protein release by using reduction-responsive nanoparticles that were bound to the plasma membrane of T cells (**Fig. 1c**). To this end we generated a 'carrier-free' protein backpack (**Fig. 1d**): We synthesized a disulphide-containing bis-*N*-hydroxy succinimide (NHS) cross-linker (NHS-SS-NHS) and identified conditions in which the solution-phase reaction of cross-linker and cargo proteins led to the formation of NGs comprised of many copies of the protein that were cross-linked to itself. NG formation typically required a large molar excess of cross-linker to protein (for example, 15:1 cross-linker:protein; **Supplementary Fig. 2a**). NGs formed from several proteins, including cytokines and antibodies, contained a high mass fraction of protein cargo (~92% of dry weight) with a high incorporation efficiency (>90%, **Supplementary Table 1**), were relatively homogeneous (~80–130 nm mean hydrodynamic diameters) (**Fig. 1e**,**f**) and had slightly negative zeta potentials (**Supplementary Table 2**). The disulphide cross-linker was designed to be cleaved in response to reducing conditions at the T cell surface, followed by release of un-adducted protein cargo through a self-immolative reaction (**Fig. 1d**)[17–19]. For promising therapeutic cargos, we focused our efforts on IL-2Fc (a fusion protein between IL-2 and an antibody Fc fragment) and ALT-803, a human IL-15 superagonist complex (IL-15Sa) that is presently in clinical trials against hematological malignancies and solid tumors[5,20,21]. Consistent with expectations, reducing agents, such as glutathione (GSH), accelerated the release of IL-15Sa from NGs in a manner dependent on the NG cleavable disulphide (**Fig. 1g** and **Supplementary Fig. 2b**). Cytokine released from the NGs exhibited the expected molecular weight and had bioactivity indistinguishable from that of unmodified IL-15Sa (**Fig. 1h** and **Supplementary Fig. 2c**), suggesting that there was release of intact cytokine without extensive residual chemical groups.

CD45 maintains nanogels at the cell surface

To sustain stimulation, NG backpacks must not be internalized by the carrier cell. We initially attempted to link NGs to T cells through the incorporation of maleimide- or NHS-activated cross-linkers into the NG structure, for covalent coupling to free thiols or amines on cell surface proteins (**Supplementary Fig. 3**). This approach, which was previously successful for the attachment of lipid nanocarriers with encapsulated drug cargos, led to rapid internalization of the IL-2Fc or IL-15Sa NGs (**Fig. 2a**). Endocytosis was not observed with control NGs that were formed with albumin (**Fig. 2a**), suggesting that internalization was a result of cell surface cytokine receptor binding to the cytokine-NG even before protein was released and the triggering of natural internalization pathways for these cytokines[22].

To increase the cell surface half-life of the NGs, we used monoclonal-antibody-functionalized liposomes to screen for slowly internalizing T cell surface proteins that could be used as specific anchors for the NGs. We tested targeting to CD2, CD8, CD11α, CD90 and CD45, candidate receptors we had previously identified in a mass spectrometry analysis of proteins that stably anchored lipid nanocapsules to T cells using maleimide chemistry[12]. We incubated T cells with antibody- and biotin-functionalized liposomes and measured the fraction of surface-accessible vesicles over time. Liposomes that were targeted to most of these receptors showed substantial internalization within a few days, with the exception of those that targeted CD45, which exhibited prolonged cell surface retention (**Fig. 2b**). Free anti-CD45 also exhibited a long cell surface half-life when bound in excess to T cells (**Supplementary Fig. 4a**). IL-2Fc-conjugated liposomes, which exhibited rapid internalization, could be stably retained on the cell surface if they were additionally functionalized with a small quantity of anti-CD45 (**Fig. 2c**,**d**). Cross-linking of CD45 via anti-CD45-bearing particles did not inhibit T cell proliferation in response to anti-CD3/CD28 beads (**Supplementary Fig. 4b**), suggesting that CD45 binding did not inhibit TCR signaling.

Guided by these findings, we incorporated a small quantity of anti-CD45 into the NGs (10 mol % relative to the IL-15Sa payload) to provide noncovalent attachment of the NGs to cells (**Fig. 2e**). We also adsorbed a small quantity of poly(ethylene glycol)-*b*-poly(L-lysine) (PEG-PLL) to the NGs immediately following the synthesis reaction. Covalent coupling of a portion of PEG-PLL to residual cross-linker NHS groups at the particle surfaces provided a uniform positive zeta potential to the particles and promoted initial electrostatic association between the particle and plasma membrane (**Fig. 2e**), maximizing the efficiency and total amount of NG loading per cell (**Supplementary Tables 2** and **3**). With this approach, T cells could be homogeneously loaded with a desired dose of cytokine-NGs, up to ~8 μg IL-15Sa per 10^6 T cells (**Fig. 2f** and **Supplementary Table 3**). Cytokine-NGs containing anti-CD45 were retained on the surfaces of unstimulated T cells for at least 7 d (**Fig. 2g**,**h**). An analogous approach using anti-human-CD45-specific antibodies (anti-hCD45) led to similar cell surface retention of NGs on human CD8$^+$ T cells (**Supplementary Fig. 5**). Anti-CD45/protein-NGs coupled to primed T cells released protein much faster when the cells were stimulated with anti-CD3/CD28 beads or peptide-pulsed dendritic cells (**Fig. 2i**,**j** and **Supplementary Fig. 6a**,**b**). Finally, because a portion of activated effector T cells might be expected to undergo apoptosis *in vivo* as part of their normal fate, we tested whether cell death would cause acute release of NG payloads that might lead to toxicity. As shown in **Supplementary Figure 6c**,**d**, induction of apoptotic cell death in backpacked T cells using anti-CD95 led to no loss of NGs over several hours, suggesting there were no dramatic changes in cell-bound NGs on dying cells.

Cytokine NGs promote enhanced T cell expansion *in vitro*

T cells that were backpacked with anti-CD45- and IL-15Sa-containing NGs (hereafter referred to as 'aCD45/IL-15Sa-NGs') and stimulated with anti-CD3/CD28 beads expanded ~100-fold in 5 d, a substantial increase relative to T cells that had been pulsed with the same total amount of free IL-15Sa for 1 h and then washed out. There were also more backpacked T cells than cells that had been cultured continuously with IL-15Sa, suggesting that cell surface localization of the NGs enhanced receptor engagement (**Fig. 3a**,**b**). NGs that were linked to T cells covalently rather than via anti-CD45 (which we refer to as 'IL-15Sa-NGs') and NGs that were formed with a non-degradable cross-linker (hereafter referred to as 'aCD45/IL-15Sa-NGs (non-deg.)') stimulated weaker T cell expansion than redox-responsive aCD45/IL-15Sa-NGs (**Fig. 3a**), suggesting that both stable cell surface retention and release of cytokine from NGs were important for maximal stimulation. Attachment of aCD45/IL-15Sa-NGs to purified polyclonal CD4$^+$ and CD8$^+$ T cells showed similar responsiveness of both T cell subsets to nanogel-promoted expansion (**Supplementary Fig. 7a**). To assess the impact of a delay between T cell preparation–backpacking

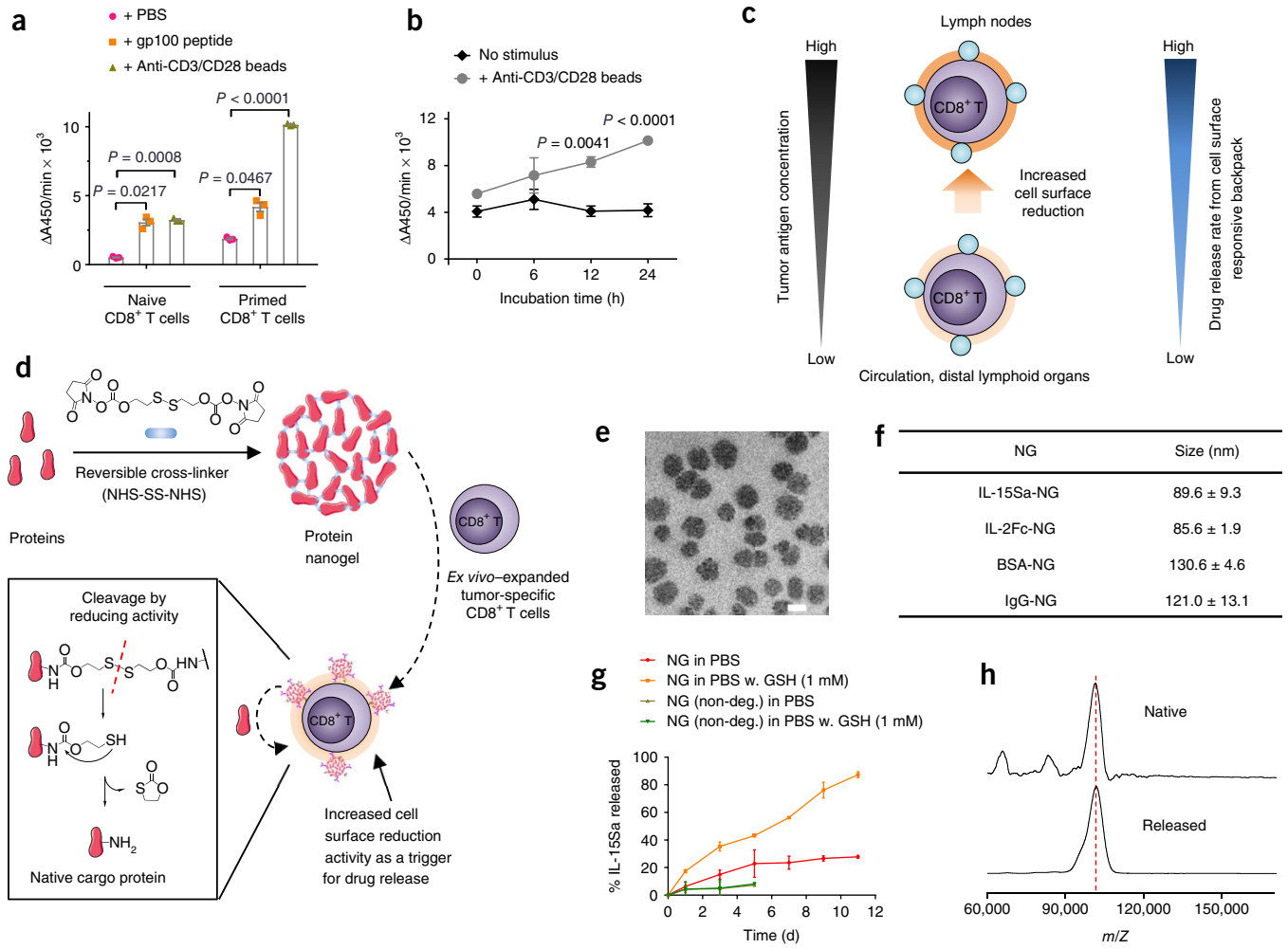

Figure 1 Synthesis and characterization of TCR-signaling-responsive protein nanogels. (**a**) Measurement of WST-1 cell-surface reduction activity rate in the presence of an intermediate electron acceptor for 1 h at 37 °C after naive or con-A-primed CD8⁺ T cells were incubated in the presence of gp100 peptide (10 μg/ml) or anti-CD3/CD28 beads for 24 h. (**b**) Cell surface reduction activity rate in con-A-primed CD8⁺ T cells that were incubated in the presence of anti-CD3/CD28 beads. Data in **a**,**b** represent the mean ± s.e.m. ($n = 3$ biologically independent samples per group), and P values were determined by one-way analysis of variance (ANOVA) and Tukey's tests. (**c**) Proposed strategy for linking increased surface redox activity of activated CD8⁺ T cells to accelerated drug release kinetics from a redox-responsive backpack. (**d**) Scheme for protein NG synthesis and for release of protein in response to reducing activity in the local microenvironment. (**e**) Representative transmission electron microscopy image of NGs prepared from IL-15Sa ($n = 3$ independent experiments). Scale bar, 50 nm. (**f**) Hydrodynamic sizes of different NGs, as determined by dynamic light scattering ($n = 3$ independent samples). Data are mean ± s.d. (**g**) Release kinetics of cytokines from redox-responsive or nondegradable IL-15Sa-NGs in PBS with or without added glutathione (GSH) as a reducing agent. Data are mean ± s.d. ($n = 3$ independent experiments). (**h**) Representative MALDI mass spectrometric analysis of released and native cytokines ($n = 2$ independent experiments).

and engagement with antigen in tumors, we tested the effect of incubating backpacked T cells with IL-7 (to maintain T cell viability during the incubation) for 3 d before TCR stimulation. With delayed stimulation, NGs still expanded the T cells *in vitro*, though to a lesser degree than that with cells stimulated immediately (**Supplementary Fig. 7b**). NGs enhanced T cell proliferative responses to anti-CD3/CD28 beads at doses as low as ~30 ng IL-15Sa per 10^6 cells (**Fig. 3c**). IL-15Sa-backpacked T cells maintained approximately constant levels of IL-15Rβ (CD122) and maintained stimulation of T cells for at least a week in culture, as evidenced by elevated levels of pSTAT5 and Ki67 over a 9-d period (**Fig. 3d**). Addition of a CD45 inhibitor did not alter the proliferative response to the NGs (**Supplementary Fig. 8**), indicating that NG anchoring did not trigger suppressive CD45 phosphatase activity.

T cell expansion in tumors

We next investigated the effect of NG-mediated cytokine delivery on ACT T cell expansion *in vivo*, via adoptive transfer of pmel-1 TCR-transgenic gp100-specific T cells[23] carrying aCD45/IL-15Sa-NGs in the syngeneic mouse model of B16F10 melanoma[5]. C56Bl/6 mice with established subcutaneous (s.c.) B16F10 flank tumors were lymphodepleted, then received intravenous (i.v.) adoptive transfer of primed pmel-1 Thy1.1⁺CD8⁺ T cells, followed by i.v. injection of 40 μg free IL-15Sa or of aCD45/IL-15Sa-backpacked T cells at the same cytokine dose (**Fig. 4a**). Seven days later, tissues were analyzed by flow cytometry, using Thy1.1 expression to distinguish ACT versus endogenous CD8⁺ T cells (**Fig. 4b**). ACT adjuvanted by free systemic IL-15Sa led to substantial expansion of both transferred pmel-1 T cells and endogenous T cells in the blood (**Fig. 4c**), and it also expanded NK cells and CD4⁺ T cells

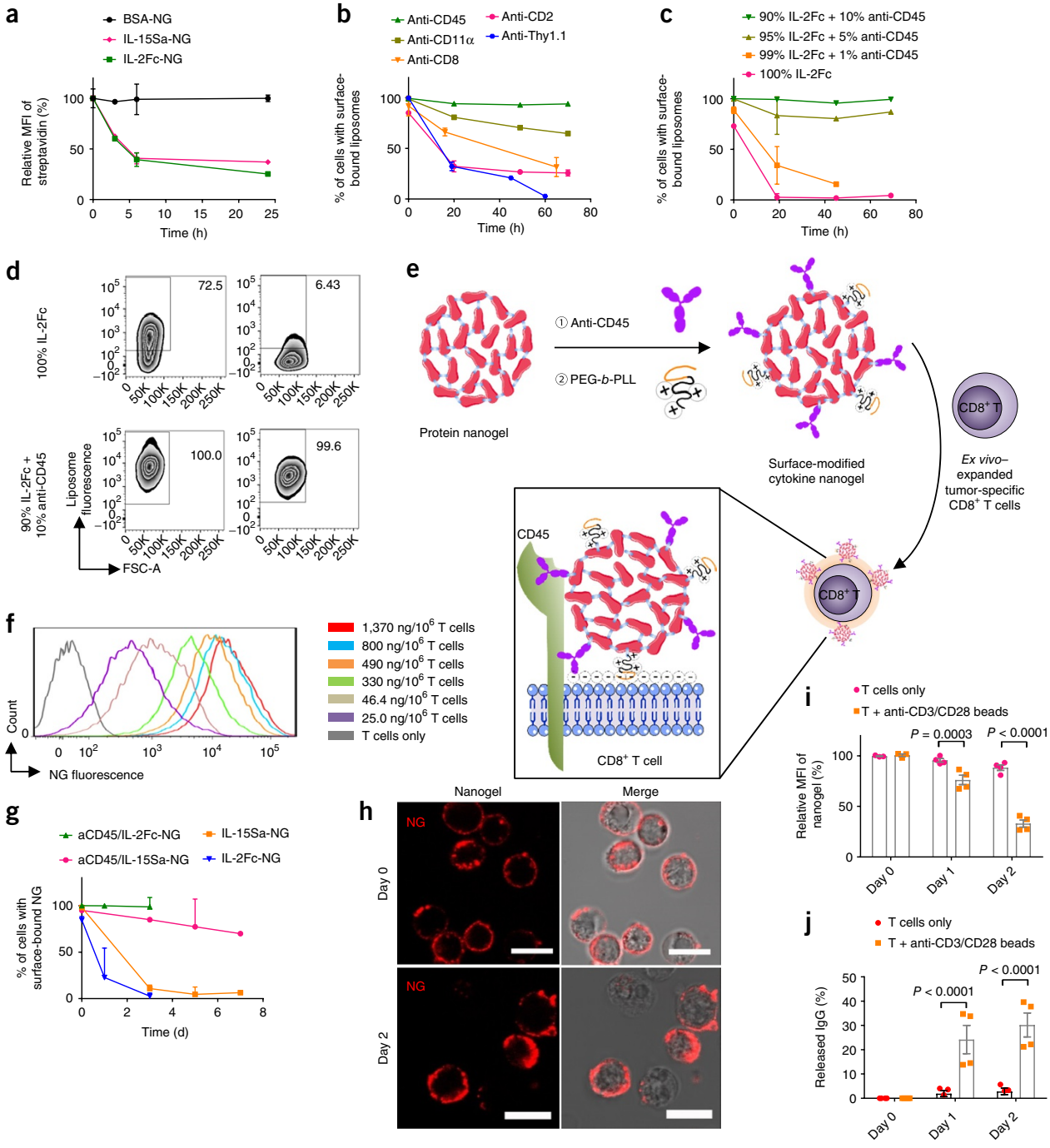

Figure 2 Nanogel anchoring to CD45 promotes prolonged cell surface retention. (**a**) Flow cytometric analysis of biotinylated protein NGs that were covalently coupled to primed pmel-1 CD8⁺ T cells via a bis-NHS cross-linker, incubated in medium for the indicated amounts of time and stained with fluorescent streptavidin (SAv) to detect cell-surface-accessible particles ($n = 3$ independent samples per group). MFI, mean fluorescence intensity. (**b**–**d**) Flow cytometric analysis of biotinylated liposomes that were functionalized with the indicated monoclonal antibodies (**b**) or a mixture of anti-CD45 and IL-2Fc (**c**,**d**), incubated with primed pmel-1 CD8⁺ T cells for the indicated amounts of time, stained with fluorescent SAv and analyzed by flow cytometry to measure cell-surface-accessible liposomes. Shown are the mean percentage of cells with surface-accessible liposomes (**b**,**c**) and representative flow cytometry plots showing the frequencies of cells with surface-bound liposomes at 0 h (left) and 19 h (right) after incubation (**d**) ($n = 3$ independent samples per group). FSC-A, forward scatter. (**e**) Scheme for surface modification of cytokine-NGs to facilitate efficient and stable anchoring on T cell surfaces. (**f**) Representative flow cytometric analysis of NG levels on primed pmel-1 CD8⁺ T cells that were coupled with fluorescently labeled aCD45/IL-15Sa NGs at the indicated cytokine levels ($n = 3$ independent experiments). (**g**) Flow cytometric analysis of primed pmel-1 CD8⁺ T cells that were conjugated with biotinylated aCD45/cytokine-containing or cytokine-only-containing NGs, incubated for the indicated amounts of time and stained with SAv for analysis of cell-surface NGs ($n = 3$ independent samples per group). (**h**) Representative confocal microscopy images of primed pmel-1 CD8⁺ T cells with fluorescently labeled aCD45/IL-15Sa-NGs (red) on day 0 and day 2 ($n = 3$ independent experiments). Scale bars, 10 μm. (**i**,**j**) Release of fluorescently labeled IgG from aCD45/IgG-NGs attached to primed pmel-1 CD8⁺ T cells incubated with or without anti-CD3/CD28 beads as assessed by flow cytometry (**i**) and HPLC analysis (**j**) of culture supernatants ($n = 4$ independent samples per group). Throughout, data represent the mean ± s.e.m., and P values were determined by one-way ANOVA and Tukey's tests.

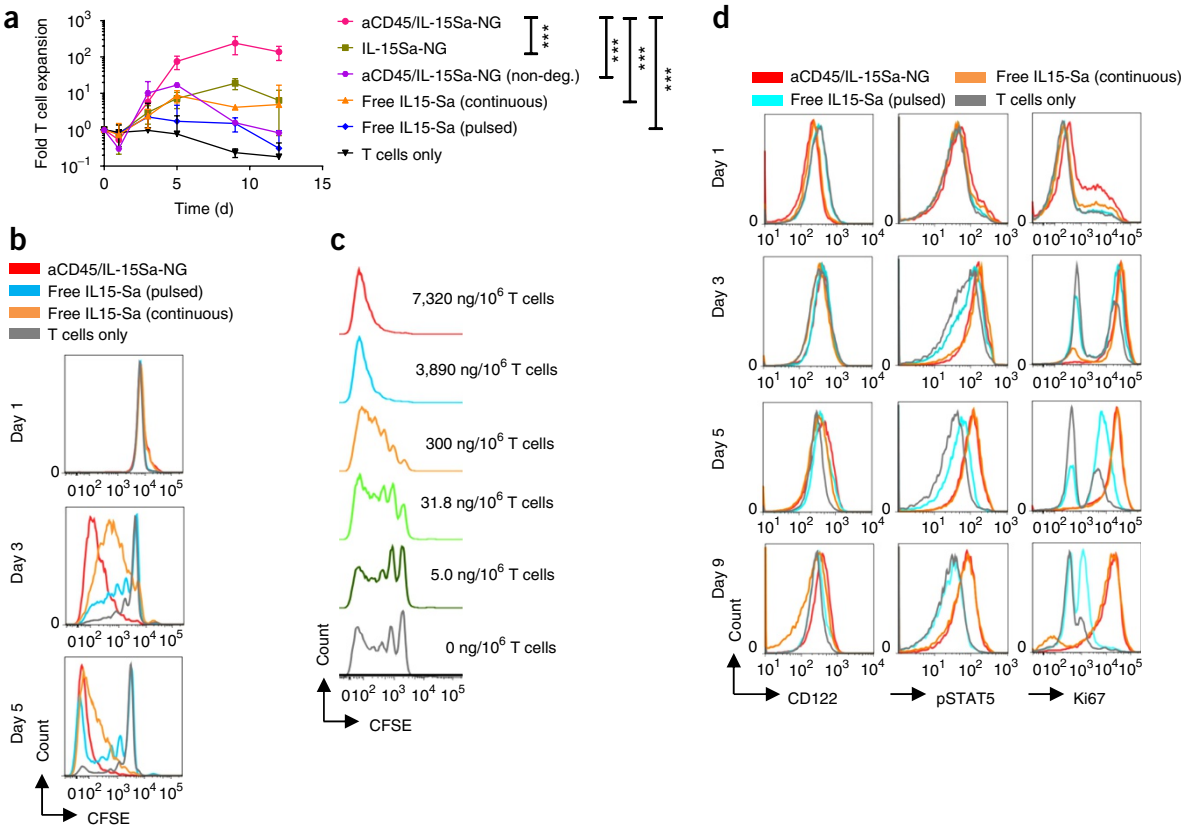

Figure 3 IL-15Sa-NG backpacks promote T cell expansion *in vitro*. (**a**) Fold expansion of naive CD8$^+$ T cells that were stimulated with anti-CD3/CD28 beads in the presence of surface-bound aCD45/IL-15Sa-NGs (7.5 μg IL-15Sa per 10^6 cells), IL-15Sa-NGs or nondegradable NGs (aCD45/IL-15Sa-NGs(non-deg.)) or that were incubated with free IL-15Sa at equivalent doses with either a pulse for 1 h or continuous cultured with the same cytokine for 12 d. Data represent the mean ± 95% confidence interval (CI) ($n = 3$ independent samples), and P values were analyzed by one-way ANOVA and Tukey's tests (data at day 9). ***$P < 0.0001$. (**b**) Representative flow cytometric analysis of carboxyfluorescein succinimidyl ester (CFSE)-labeled naive pmel-1 CD8$^+$ T cells that were stimulated with anti-CD3/CD28 beads in the presence of surface-bound aCD45/IL-15Sa-NGs (7.5 μg IL-15Sa per 10^6 T cells) or that were incubated with an equivalent amount of free IL-15Sa for the indicated amounts of time ($n = 3$ independent experiments). (**c**) Representative profiles showing CFSE dilution of naive pmel-1 CD8$^+$ T cells that were stimulated with anti-CD3/CD28 beads in the presence of various densities of surface-bound aCD45/IL-15Sa-NGs ($n = 3$ independent experiments). (**d**) Representative flow cytometric analysis of levels of the IL-15 surface receptors, the phosphorylated form of the transcription factor STAT5 (pSTAT5) and the proliferation marker Ki67 in naive pmel-1 CD8$^+$ T cells that were stimulated with anti-CD3/CD28 beads in the presence of surface-bound aCD45/IL-15Sa-NGs (7.5 μg IL-15Sa per 10^6 cells) or that were incubated with an equivalent amount of free IL-15Sa over 9 d ($n = 3$ independent experiments).

in the systemic circulation (**Supplementary Fig. 9**). Systemic IL-15Sa treatment also expanded endogenous T cells in tumor-draining lymph nodes (TDLNs) and tumors (**Fig. 4d–f**). By contrast, IL-15Sa delivered as backpacks expanded the transferred CD8$^+$ T cells but did not expand endogenous T cells in any compartment (**Fig. 4c–f**). This lack of bystander stimulation was consistent with control experiments in which we assessed the transfer of labeled NGs to endogenous innate or adaptive cells in the blood 2 d after injecting backpacked pmel-1 cells; only a very minor population of endogenous CD8$^+$ T cells (≤1.3%) was found to acquire NG fluorescence (**Supplementary Fig. 10**). In tumors, where we expected antigen recognition to accelerate IL-15Sa release from the NGs, there was a 16-fold greater expansion of IL-15Sa-backpacked T cells than pmel-1 T cells in the soluble IL-15Sa-adjuvanted group and 1,000-fold greater expansion than the T cells without cytokine support (**Fig. 4b**,**f**). After ranking tissues in the order of expected increasing antigen concentration (blood < distal LN < TDLN < tumor), we observed a corresponding increasing ratio of ACT T cell counts in the NG group versus the ACT cells in the free IL-15Sa-adjuvanted group (**Fig. 4g**). Backpacked T cells in the tumor were also still proliferating and producing granzyme and effector cytokines (**Fig. 4h–j**). Further evidence for the antigen-driven stimulation by the NG backpacks came from a comparison of T cell expansion in tumor-bearing versus control non-tumor-bearing mice. As shown in **Supplementary Figure 11**, at day 3 post transfer, T cells were already expanded by NGs in tumors, but not in distal LNs or LNs of non-tumor-bearing mice; by contrast, systemic IL-15Sa treatment resulted in a modest expansion of T cells in the LNs of both groups. Unlike TCR-triggered T cells, B16F10 cells showed no extracellular reducing activity (**Supplementary Fig. 12**), suggesting that cytokine release in the tumors was mediated by T cell surface redox rather than by a reducing microenvironment in the tumors. NG IL-15Sa delivery thus focused cytokine action on the transferred T cells, and preferentially in antigen-bearing microenvironments *in vivo*.

Increased therapeutic window for adjuvant cytokine therapy

We noted that mice that received free high-dose IL-15Sa lost weight following therapy, which prompted us to explicitly evaluate the toxicity of IL-15Sa as a function of dose and delivery modality. We treated

tumor-bearing mice with pmel-1 T cells and IL-15Sa in different dosing schemes (**Fig. 5a**). Mice that received >10 μg of free IL-15Sa steadily lost weight and eventually succumbed to lethal immunotoxicity irrespective of dosing regimen, setting the maximum tolerated dose (MTD) at 10 μg in this model (**Fig. 5b**). In contrast, when administered in the form of T cell-bound NGs, no overt toxicity was observed

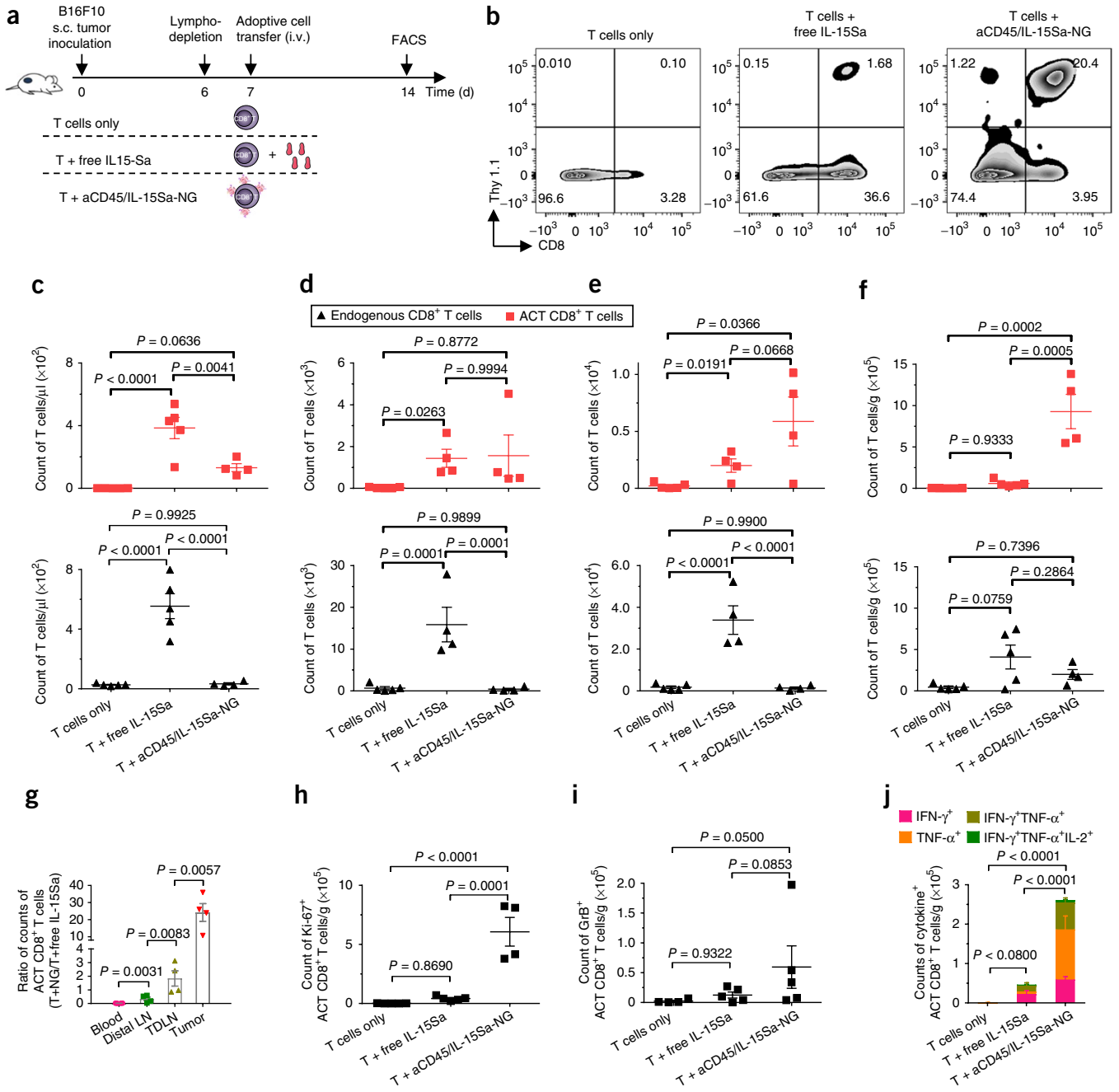

Figure 4 IL-15Sa-NGs promote specific expansion of adoptively transferred T cells in tumors. B16F10 tumor cells (0.5×10^6) were subcutaneously administered to Thy1.2+ C57Bl/6 mice and allowed to establish for 6 d. Mice were then sublethally lymphodepleted by irradiation on day 6, and were intravenously administered 10×10^6 primed pmel-1 Thy1.1+CD8+ T cells on day 7. Treatment groups included T cells alone, T cells followed by a systemic injection of free IL-15Sa (40 μg) and T cells coupled with aCD45/IL-15Sa-NGs (40 μg). On day 14, mice were euthanized, and tissues were processed and analyzed by flow cytometry ($n = 4$ mice/group). (**a**) Experimental timeline. (**b**) Representative flow cytometry plots showing the frequencies of tumor-infiltrating Thy1.1+CD8+ T cells among all of the lymphocytes. (**c**–**f**) Counts of adoptively transferred (ACT) Thy1.1+CD8+ T cells (red squares) and endogenous Thy1.1−CD8+ T cells (black triangles) in blood (**c**, normalized by volume), non-TDLNs (**d**, distal LNs), TDLNs (**e**) and tumors (**f**, normalized by weight). (**g**) Ratios of counts of ACT CD8+ T cells in the group of T + aCD45/IL-15Sa-NG relative to that of T + free IL-15Sa in different tissues. (**h**) Counts of Ki67+ ACT CD8+ T cells in tumors, as analyzed by intracellular staining and flow cytometry. (**i**) Counts of granzyme-B+ ACT CD8+ T cells in tumors, as analyzed by intracellular staining and flow cytometry on day 10 ($n = 5$ mice/group). (**j**) Counts of polyfunctional ACT CD8+ T cells in tumors, as assessed by intracellular cytokine staining. Throughout, data represent the mean ± s.e.m., and *P* values were determined by one-way ANOVA and Tukey's tests. All data are one representative of at least two independent experiments.

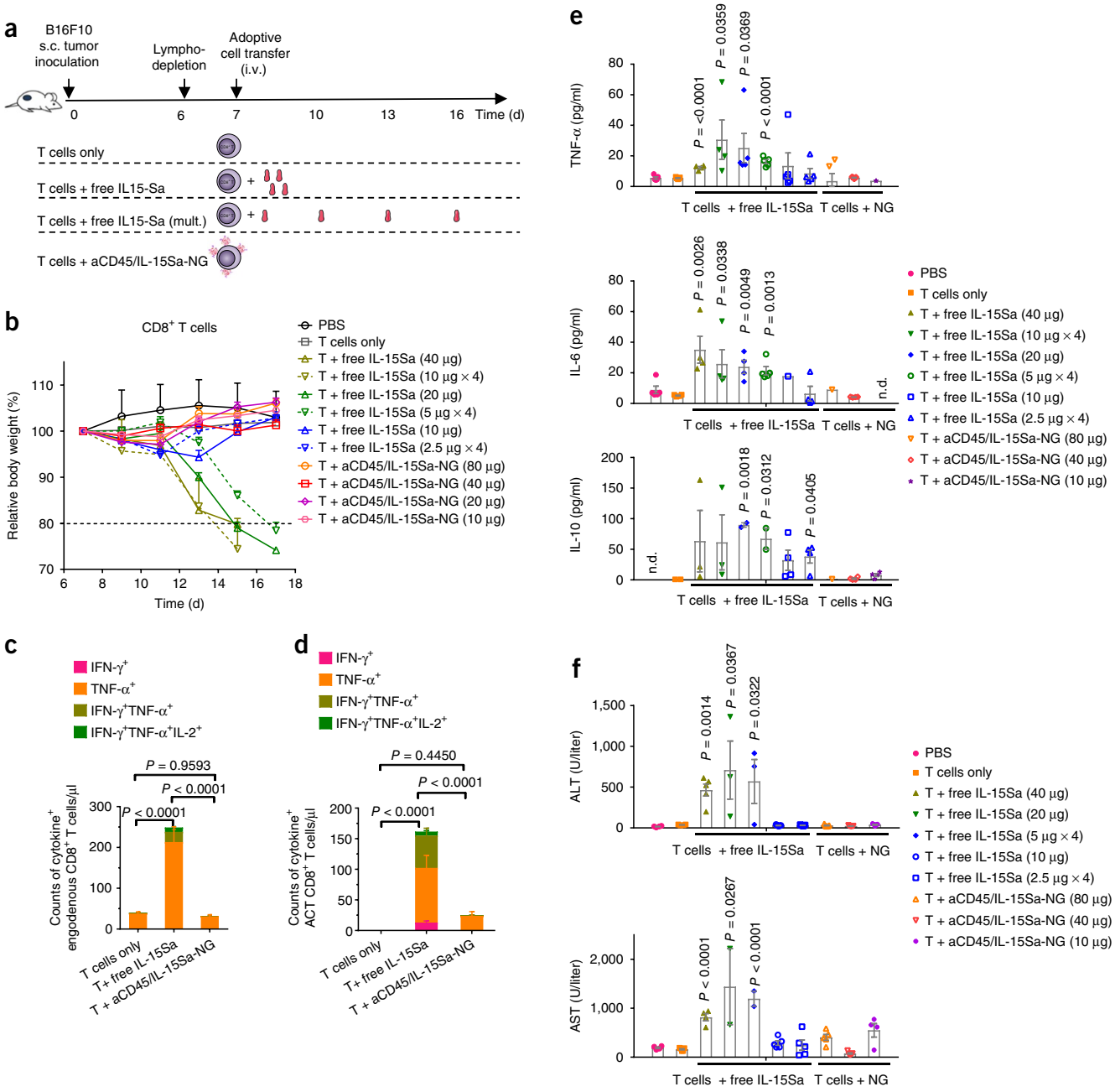

Figure 5 IL-15Sa-NG backpacks increase the therapeutic window for adjuvant cytokine delivery during ACT. B16F10 tumor cells (0.5×10^6) were injected subcutaneously in Thy1.2+ C57Bl/6 mice and allowed to establish tumor for 6 d. Mice were then sublethally lymphodepleted by irradiation on day 6, and they intravenously received an adoptive transfer of 10×10^6 activated pmel-1 Thy1.1+CD8+ T cells on day 7. Mice received injections of PBS (sham), T cells only, T cells followed by different doses of intravenously injected free IL-15Sa either as a single dose (immediately after adoptive transfer) or split into multiple doses (days 7, 10, 13 and 16), or T cells backpacked with aCD45/IL-15Sa-NG at different doses. Body weights and systemic cytokine, chemokine and liver enzyme levels were analyzed over time. (**a**) Experimental timeline and groups. (**b**) Body weight, normalized to that for day 7, over time for the different treated groups. (**c**–**e**) Counts of cytokine+ endogenous CD8+ T cells (**c**) and ACT CD8+ T cells (**d**) in blood, as analyzed by intracellular cytokine staining and flow cytometry. (**e**,**f**) Serum cytokine levels (**e**) and liver enzymes (**f**) were measured from samples collected on day 17 or when the mice were euthanized due to toxicity. Throughout, data represent the mean ± s.e.m. ($n = 5$ mice/group) and were compared with the control group (T cells only) for statistical analyses by using one-way ANOVA and Tukey's tests; n.d., not detectable. Shown is one representative of two independent experiments.

up to the maximum achievable IL-15Sa loading per cell (80 µg IL-15Sa per 10×10^6 T cells; **Fig. 5b**). Treatment with free IL-15Sa stimulated cytokine production from both pmel-1 and endogenous T cells in the blood, in contrast to IL-15Sa that was delivered by NGs, for which the majority of both backpacked and endogenous T cells remained quiescent in the systemic circulation (**Fig. 5c**,**d**). This lack of systemic stimulation correlated with low levels of detectable free IL-15Sa in the blood for backpacked T cells, even when much higher

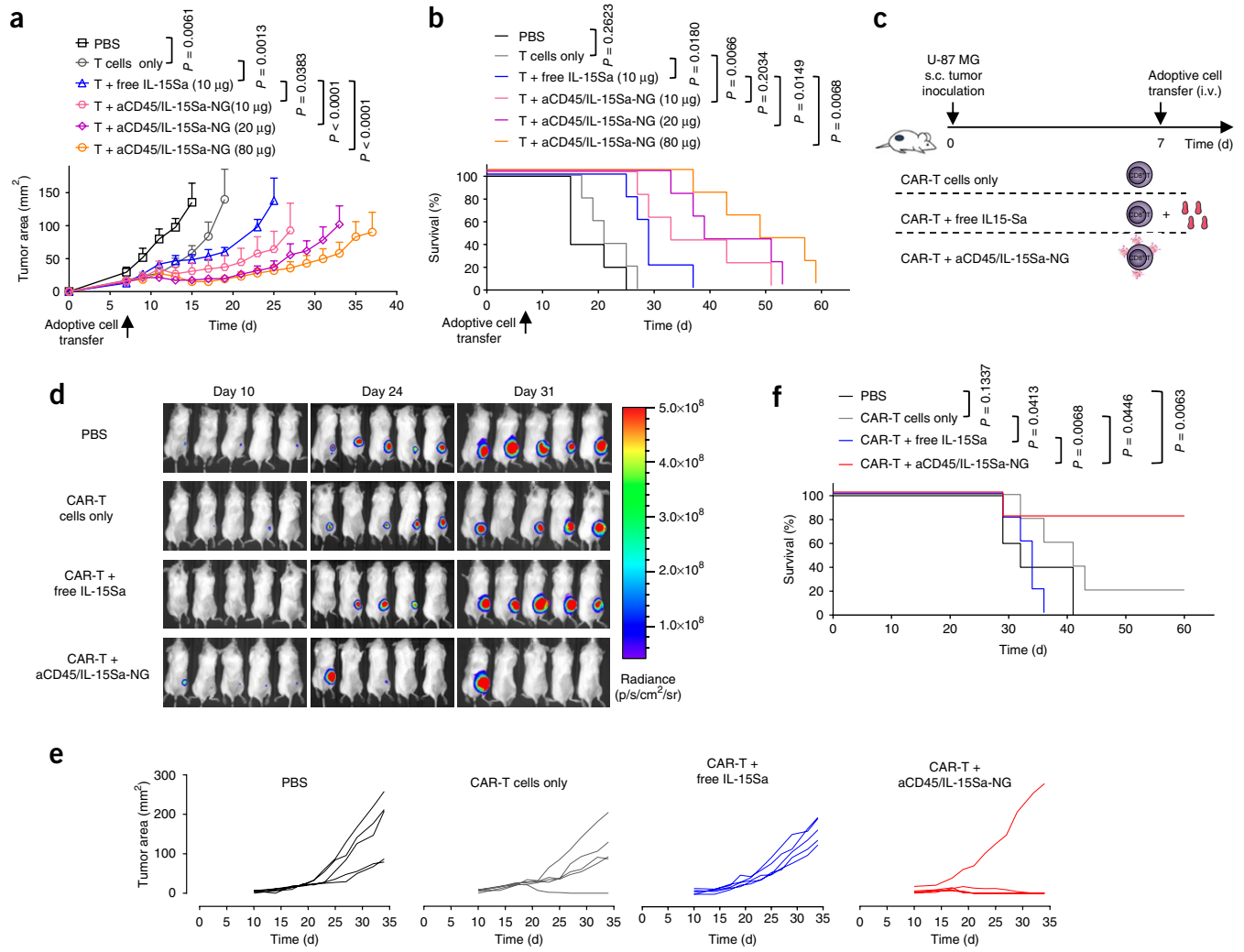

Figure 6 TCR signaling–responsive NG backpacks improve T cell therapies. (**a**,**b**) B16F10 tumor cells (0.5×10^6) were injected subcutaneously in Thy1.2+ C57Bl/6 mice ($n = 5$ mice/group) and allowed to establish for 6 d. Mice were then sublethally lymphodepleted by irradiation on day 6 and intravenously administered 10×10^6 activated pmel-1 Thy1.1+CD8+ T cells on day 7. Mice received injections of PBS (sham), T cells only, T cells with 10 μg intravenously injected free IL-15Sa or aCD45/IL-15Sa-NG-backpacked T cells at the indicated IL-15Sa doses. Shown are average tumor growth curves (**a**) and survival curves (**b**) of each treatment group. (**c**) Experimental scheme. Luciferase-expressing U-87 MG human glioblastoma cells (1.0×10^6) were subcutaneously injected into NSG mice ($n = 5$ mice/group). Mice received i.v. adoptive transfer of human T cells (2.6×10^6 total cells, 38% transduced with EGFR-targeting CAR (1.0×10^6 CAR-T cells)) on day 7. Mice were treated with sham saline injections, CAR-T cells alone, CAR-T cells followed by 13.8 μg of free IL-15Sa, or CAR-T cells coupled with aCD45/IL-15Sa-NGs (13.8 μg). (**d**) *In vivo* bioluminescence imaging of luciferase-expressing U-87 MG tumors over time, as outlined in **c**. (**e**,**f**) Individual tumor growth curves (**e**) and survival curves (**f**) of treatment groups, as outlined in **c**. Statistical analyses were performed by using two-way ANOVA test for tumor growth data and log-rank test for survival curves. Data represent the mean ± s.e.m. All data are one representative of at least two independent experiments.

total doses of cytokine were administered as compared to that with the soluble bolus injections (**Supplementary Fig. 13a**). In healthy mice, treatment with >10 μg free IL-15Sa did not elicit high levels of serum cytokine induction[21]. However, in this lymphodepletion setting, ACT with >10 μg free IL-15Sa induced systemic cytokine release and elevated levels of liver enzymes (**Fig. 5e**,**f** and **Supplementary Fig. 13b**), whereas backpacked T cells elicited basal levels of these biomarkers after treatment with up to the maximum administrable dosage.

To determine the effect of the increased therapeutic window afforded by IL-15Sa-NGs, we compared the antitumor efficacy of ACT with T cells only, with T cells and free IL-15Sa (at the MTD of 10 μg) or with NG-backpacked T cells following the same treatment scheme as that in **Figure 5a**. Tumor growth was substantially delayed in the 10 μg IL-15Sa-NG group as compared to that in the T cell group with free IL-15Sa support at the same dose (**Fig. 6a**). However, tumor suppression was further enhanced by increasing the cytokine-NG dose, with animals treated at the maximal 80 μg dose showing a 1.7-fold increase in median survival time relative to animals that were treated with the MTD of free IL-15Sa (**Fig. 6a**,**b**). Notably, despite the use of a xenogeneic (human) IL-15Sa cytokine, no hIL-15Sa-specific antibodies (relative to background) were detected in serum following treatment in any of the NG-backpack-treated groups (**Supplementary Fig. 14**). We also compared NG-mediated IL-15 delivery to the cytokine-loaded multilamellar lipid capsules that were used in our first report of the backpacking approach[11] and found that even when administered at the same total cytokine dose, IL-15-NGs elicited much

greater T cell expansion in tumors and greater tumor regression than that with lipid nanocapsule backpacks (**Supplementary Fig. 15**). The lack of toxicity associated with NG–T cell transfer allowed us to achieve further antitumor efficacy by administering multiple injections of backpacked T cells. Administration of a second dose of NG–T cells 1 week after the first injection led to greatly improved survival and cures in 60% of treated mice, whereas systemic IL-15Sa treatment and T cells dosed twice resulted in toxicity (**Supplementary Fig. 16**).

Finally, we evaluated whether NG-delivered cytokine could also positively impact the function of CAR-T cells, which are an important modality of T cell therapy in the clinic[4]. For this purpose, we used human CAR-T cells that targeted epidermal growth factor receptor (EGFR) in a luciferase-expressing human glioblastoma model in immunodeficient NSG mice (**Fig. 6c**). CAR-T cells that were maximally backpacked with IL-15Sa-NGs were compared to CAR-T cells alone or CAR-T cells supplemented with an equivalent systemic dose of free IL-15Sa. Transfer of 10^6 CAR-T cells had a small effect on tumor growth and survival, which did not reach statistical significance; responses were marginally improved by the addition of free IL-15Sa (**Fig. 6d–f**). By contrast, NG-backpacked CAR-T cells eradicated tumors in four of five mice (**Fig. 6d–f**). We also found that frozen NG-loaded CAR-T cells retained the ability for cytokine-driven expansion after thawing (**Supplementary Fig. 17**), a property that may be helpful for clinical protocols that use cryopreserved T cell products. Thus, NG delivery of cytokines also has the potential to enhance CAR-T cell therapy.

DISCUSSION

ACT has recently achieved notable clinical responses in certain hematological cancers[24]. However, ACT for solid tumors has remained challenging, at least in part due to the immunosuppressive tumor microenvironment[1,25]. The administration of immunomodulators might overcome this microenvironment, but these drugs are often limited by systemic toxicities[7,26]. Here we demonstrated a chemical strategy to increase the efficacy and safety of adjuvant drug therapy for ACT, by linking drug delivery to TCR triggering in the tumor and TDLNs.

Two biological discoveries enabled this approach. First, we found that T cells modulate their cell surface redox state as a function of activation status (naive versus primed cells) and immediately following TCR–cognate-peptide–MHC engagement. The mechanisms underlying this redox regulation remain to be defined, but they may involve altered expression of transmembrane reducing enzymes. The second key finding was the identification of CD45 as a stable, non-internalizing anchor for NGs, even when the particles exposed protein ligands that normally trigger endocytosis. Prior studies reported that CD45-targeted nano-emulsions are endocytosed after binding to CD45 expressed by murine macrophages[27], suggesting that binding to CD45 may have different outcomes in different immune cell populations. Biochemical studies in Jurkat T cells also reported a half-life for cell-surface CD45 of 6–15 h[28], which may reflect the distinct behavior of free versus particle-cross-linked CD45 and/or differences in the biology of primary T cells and cell lines. Although CD45 plays important roles in regulating T cell signaling at the immunological synapse[29,30], anchoring of NGs to CD45 did not affect proliferative responses to TCR–cytokine stimuli.

The identification of reaction conditions that yielded discrete nanoparticles through solution cross-linking of proteins was consistent with prior literature on protein micro- and nano-gels[31–33]. The NG strategy enabled high per-cell doses of protein to be delivered; by comparison, measurements of maximal T cell loading with a CD45-specific monoclonal antibody suggested that use of an anti-CD45–cytokine fusion as an alternative could achieve at best a 70-fold lower maximal cytokine payload.

By using TCR-responsive NGs, we reduced to practice an approach of spatiotemporally controlled drug delivery, linking tissue-specific cell signaling (here, antigen recognition) to drug release. The cross-linker system we used responded to local changes in the redox environment, and although some tumors are thought to intrinsically present a reducing state, melanomas, by contrast, have been shown to generate an oxidative microenvironment[34]. We detected no extracellular reducing activity in B16F10 tumor cells that were assayed immediately after removal from established tumors, which suggested that cytokine release from the backpacks was primarily driven by T cell–mediated cell surface reduction. However, we can also envision NGs that are responsive to the dysregulated physiology of the tumor microenvironment itself. Tumors are often hypoxic, acidic and overexpress various proteases[35]. Numerous environment-responsive chemistries have been developed in the drug delivery field to achieve tissue-selective drug release—for example, particles responsive to tumor-enriched matrix metalloproteinases[36], to acidic pH[37,38] or to other signals[35,39]. Implementation of these approaches in the NG cross-linker to impart responsiveness to cell surface enzymes, tumor-specific proteases or pH are a possibility.

This chemical strategy complements genetic engineering approaches to control the location and timing of ACT T cell activation and expansion. Safe delivery of cytokine support is also being pursued by linking cytokine expression to TCR-signaling-regulated transcription factors[40–42] and by expressing membrane-bound cytokines[43]. These and other[44–47] elegant genetic approaches promote spatiotemporal control over CAR-T cell activity. However, chemical backpacking may be more effective with cytokines that are very toxic or whose expression during *in vitro* preparation of T cells inhibits T cell expansion (for example, IL-12). A constraint of the backpacking approach is that it is an inherently self-limiting therapy, as stimulation of cell division leads to dilution of the backpacked drug cargo. This does not preclude some durability in stimulation, as evidenced by the NG backpacks that continued to stimulate T cells for at least 9 d *in vitro*. Self-limiting dosing can also be viewed as an attractive built-in safeguard against runaway stimulation of T cells or on-target–off-tumor T cell activation, which can lead to serious toxicities[9,48].

METHODS

Methods, including statements of data availability and any associated accession codes and references, are available in the online version of the paper.

Note: Any Supplementary Information and Source Data files are available in the online version of the paper.

ACKNOWLEDGMENTS

We thank K.D. Wittrup (MIT) for the gift of the engineered IL-2-Fc constructs and the Koch Institute Swanson Biotechnology Center for technical support on flow cytometry, IVIS imaging and MALDI mass spectrometry. This work was supported in part by the Ragon Institute of MGH, MIT and Harvard (D.J.I.), the Melanoma Research Alliance (award 306833; D.J.I.) , the NIH (Koch Institute Support (core) grant P30-CA14051 from the National Cancer Institute and CA172164; D.J.I.) and the Koch Institute Marble Center for Cancer Nanomedicine (D.J.I.). L.T. was funded by a Cancer Research Institute (CRI) Irvington Postdoctoral Fellowship, and Y.Z. was supported by a National Science fellowship from the Agency for Science, Technology and Research, Singapore. L.T. and Y.-Q.X. were supported by the ISREC Foundation with a donation from the Biltema Foundation and Swiss National Science Foundation (project grant 315230_173243). M.V.M. was supported by NIH grant CA K08166039. D.J.I. is an investigator of the Howard Hughes Medical Institute.

AUTHOR CONTRIBUTIONS

L.T., Y.Z., M.B.M. and D.J.I. designed the *in vitro* and syngeneic mouse experiments; H.C.W. and E.K.J. provided ALT-803; L.T., Y.Z., D.J.I., A.P.C., S.B.K.

and M.V.M. designed the studies with the humanized mice; L.T., Y.Z., L.M., M.B.M., Y.-Q.X., N.L., A.P.C. and S.B.K. performed the experiments; L.T., Y.Z., M.B.M. and D.J.I. analyzed the data and wrote the manuscript; and all authors edited the manuscript.

COMPETING INTERESTS

D.J.I., L.T., and Y.Z. are inventors on licensed patents related to the technology described in this manuscript. D.J.I. is a co-founder of Torque Therapeutics, which licensed patents related to this technology.

1. Rosenberg, S.A. & Restifo, N.P. Adoptive cell transfer as personalized immunotherapy for human cancer. *Science* **348**, 62–68 (2015).
2. Gill, S. & June, C.H. Going viral: chimeric antigen receptor T cell therapy for hematological malignancies. *Immunol. Rev.* **263**, 68–89 (2015).
3. Corrigan-Curay, J. *et al.* T cell immunotherapy: looking forward. *Mol. Ther.* **22**, 1564–1574 (2014).
4. Johnson, L.A. *et al.* Rational development and characterization of humanized anti–EGFR variant III chimeric antigen receptor T cells for glioblastoma. *Sci. Transl. Med.* **7**, 275ra22 (2015).
5. Klebanoff, C.A. *et al.* IL-15 enhances the *in vivo* antitumor activity of tumor-reactive $CD8^+$ T cells. *Proc. Natl. Acad. Sci. USA* **101**, 1969–1974 (2004).
6. Wallace, A. *et al.* Transforming growth factor–β receptor blockade augments the effectiveness of adoptive T cell therapy of established solid cancers. *Clin. Cancer Res.* **14**, 3966–3974 (2008).
7. Conlon, K.C. *et al.* Redistribution, hyperproliferation, activation of natural killer cells and CD8 T cells, and cytokine production during first-in-human clinical trial of recombinant human interleukin-15 in patients with cancer. *J. Clin. Oncol.* **33**, 74–82 (2015).
8. Leonard, J.P. *et al.* Effects of single-dose interleukin-12 exposure on interleukin-12-associated toxicity and interferon-γ production. *Blood* **90**, 2541–2548 (1997).
9. Zhang, L. *et al.* Tumor-infiltrating lymphocytes genetically engineered with an inducible gene encoding interleukin-12 for the immunotherapy of metastatic melanoma. *Clin. Cancer Res.* **21**, 2278–2288 (2015).
10. Huang, B. *et al.* Active targeting of chemotherapy to disseminated tumors using nanoparticle-carrying T cells. *Sci. Transl. Med.* **7**, 291ra94 (2015).
11. Stephan, M.T., Moon, J.J., Um, S.H., Bershteyn, A. & Irvine, D.J. Therapeutic cell engineering with surface-conjugated synthetic nanoparticles. *Nat. Med.* **16**, 1035–1041 (2010).
12. Stephan, M.T., Stephan, S.B., Bak, P., Chen, J. & Irvine, D.J. Synapse-directed delivery of immunomodulators using T cell–conjugated nanoparticles. *Biomaterials* **33**, 5776–5787 (2012).
13. Ghezzi, P., Bonetto, V. & Fratelli, M. Thiol-disulfide balance: from the concept of oxidative stress to that of redox regulation. *Antioxid. Redox Signal.* **7**, 964–972 (2005).
14. Lawrence, D.A., Song, R. & Weber, P. Surface thiols of human lymphocytes and their changes after *in vitro* and *in vivo* activation. *J. Leukoc. Biol.* **60**, 611–618 (1996).
15. Berridge, M.V. & Tan, A.S. *Trans*-plasma membrane electron transport: a cellular assay for NADH- and NADPH-oxidase based on extracellular, superoxide-mediated reduction of the sulfonated tetrazolium salt WST-1. *Protoplasma* **205**, 74–82 (1998).
16. Berridge, M.V. & Tan, A.S. Cell-surface NAD(P)H-oxidase: relationship to *trans*-plasma membrane NADH-oxidoreductase and a potential source of circulating NADH-oxidase. *Antioxid. Redox Signal.* **2**, 277–288 (2000).
17. Riber, C.F., Smith, A.A. & Zelikin, A.N. Self-immolative linkers literally bridge disulfide chemistry and the realm of thiol-free drugs. *Adv. Healthc. Mater.* **4**, 1887–1890 (2015).
18. Jones, L.R. *et al.* Releasable luciferin–transporter conjugates: tools for the real-time analysis of cellular uptake and release. *J. Am. Chem. Soc.* **128**, 6526–6527 (2006).
19. Xu, J. *et al.* Rendering protein-based particles transiently insoluble for therapeutic applications. *J. Am. Chem. Soc.* **134**, 8774–8777 (2012).
20. Zhu, X. *et al.* Novel human interleukin-15 agonists. *J. Immunol.* **183**, 3598–3607 (2009).
21. Rhode, P.R. *et al.* Comparison of the superagonist complex, ALT-803, to IL-15 as cancer immunotherapeutics in animal models. *Cancer Immunol. Res.* **4**, 49–60 (2016).
22. Yu, A., Olosz, F., Choi, C.Y. & Malek, T.R. Efficient internalization of IL-2 depends on the distal portion of the cytoplasmic tail of the IL-2R common γ-chain and a lymphoid cell environment. *J. Immunol.* **165**, 2556–2562 (2000).
23. Overwijk, W.W. *et al.* Tumor regression and autoimmunity after reversal of a functionally tolerant state of self-reactive $CD8^+$ T cells. *J. Exp. Med.* **198**, 569–580 (2003).
24. Maude, S.L. *et al.* Chimeric antigen receptor T cells for sustained remissions in leukemia. *N. Engl. J. Med.* **371**, 1507–1517 (2014).
25. Maus, M.V. *et al.* Adoptive immunotherapy for cancer or viruses. *Annu. Rev. Immunol.* **32**, 189–225 (2014).
26. Guo, Y. *et al.* IL-15 superagonist-mediated immunotoxicity: role of NK cells and IFN-γ. *J. Immunol.* **195**, 2353–2364 (2015).
27. Patel, S.K., Zhang, Y., Pollock, J.A. & Janjic, J.M. Cyclooxgenase-2 inhibiting perfluoropoly (ethylene glycol) ether theranostic nanoemulsions–*in vitro* study. *PLoS One* **8**, e55802 (2013).
28. Pradhan, D. & Morrow, J. The spectrin–ankyrin skeleton controls CD45 surface display and interleukin-2 production. *Immunity* **17**, 303–315 (2002).
29. Chang, V.T. *et al.* Initiation of T cell signaling by CD45 segregation at 'close contacts'. *Nat. Immunol.* **17**, 574–582 (2016).
30. Johnson, K.G., Bromley, S.K., Dustin, M.L. & Thomas, M.L. A supramolecular basis for CD45 tyrosine phosphatase regulation in sustained T cell activation. *Proc. Natl. Acad. Sci. USA* **97**, 10138–10143 (2000).
31. Wang, L. *et al.* Nanoclusters self-assembled from conformation-stabilized influenza M2e as broadly cross-protective influenza vaccines. *Nanomedicine (Lond.)* **10**, 473–482 (2014).
32. Scott, E.A. *et al.* Protein adsorption and cell adhesion on nanoscale bioactive coatings formed from poly(ethylene glycol) and albumin microgels. *Biomaterials* **29**, 4481–4493 (2008).
33. Tan, H. *et al.* PEG-urokinase nanogels with enhanced stability and controllable bioactivity. *Soft Matter* **8**, 2644–2650 (2012).
34. Lin, X. *et al.* Oxidative stress in malignant melanoma enhances tumor necrosis factor–α secretion of tumor-associated macrophages that promote cancer cell invasion. *Antioxid. Redox Signal.* **19**, 1337–1355 (2013).
35. Koshy, S.T., Ferrante, T.C., Lewin, S.A. & Mooney, D.J. Injectable, porous and cell-responsive gelatin cryogels. *Biomaterials* **35**, 2477–2487 (2014).
36. Singh, N. *et al.* Bioresponsive mesoporous silica nanoparticles for triggered drug release. *J. Am. Chem. Soc.* **133**, 19582–19585 (2011).
37. Au, K.M. *et al.* Folate-targeted pH-responsive calcium zoledronate nanoscale metal-organic frameworks: turning a bone anti-resorptive agent into an anticancer therapeutic. *Biomaterials* **82**, 178–193 (2016).
38. Ling, D. *et al.* pH-sensitive nanoformulated triptolide as a targeted therapeutic strategy for hepatocellular carcinoma. *ACS Nano* **8**, 8027–8039 (2014).
39. Yang, Y. *et al.* Polymer nanoparticles modified with photo- and pH-dual-responsive polypeptides for enhanced and targeted cancer therapy. *Mol. Pharm.* **13**, 1508–1519 (2016).
40. Chmielewski, M., Kopecky, C., Hombach, A.A. & Abken, H. IL-12 release by engineered T cells expressing chimeric antigen receptors can effectively muster an antigen-independent macrophage response on tumor cells that have shut down tumor antigen expression. *Cancer Res.* **71**, 5697–5706 (2011).
41. Chinnasamy, D. *et al.* Local delivery of interleukin-12 using T cells targeting VEGF receptor 2 eradicates multiple vascularized tumors in mice. *Clin. Cancer Res.* **18**, 1672–1683 (2012).
42. Pegram, H.J. *et al.* Tumor-targeted T cells modified to secrete IL-12 eradicate systemic tumors without need for prior conditioning. *Blood* **119**, 4133–4141 (2012).
43. Weinstein-Marom, H. *et al.* Membrane-attached cytokines expressed by mRNA electroporation act as potent T cell adjuvants. *J. Immunother.* **39**, 60–70 (2016).
44. Desnoyers, L.R. *et al.* Tumor-specific activation of an EGFR-targeting probody enhances therapeutic index. *Sci. Transl. Med.* **5**, 207ra144 (2013).
45. Wu, C.-Y., Roybal, K.T., Puchner, E.M., Onuffer, J. & Lim, W.A. Remote control of therapeutic T cells through a small-molecule-gated chimeric receptor. *Science* **350**, aab4077 (2015).
46. Fedorov, V.D., Themeli, M. & Sadelain, M. PD-1- and CTLA-4-based inhibitory chimeric antigen receptors (iCARs) divert off-target immunotherapy responses. *Sci. Transl. Med.* **5**, 215ra172 (2013).
47. Kloss, C.C., Condomines, M., Cartellieri, M., Bachmann, M. & Sadelain, M. Combinatorial antigen recognition with balanced signaling promotes selective tumor eradication by engineered T cells. *Nat. Biotechnol.* **31**, 71–75 (2013).
48. Morgan, R.A. *et al.* Case report of a serious adverse event following the administration of T cells transduced with a chimeric antigen receptor recognizing ERBB2. *Mol. Ther.* **18**, 843–851 (2010).

ONLINE METHODS

Materials. ALT-803, a human IL-15 super-agonist (Sa), obtained from Altor BioScience Corporation (Miramar, FL, USA) was generated as described previously[49]. IL-2-Fc, a bivalent fusion protein of the C terminus of mouse wild-type IL-2 linked to a mouse IgG2a backbone, was a generous gift from Dane Wittrup's lab at MIT and was prepared as described previously[50]. Bovine serum albumin (BSA) was purchased from Sigma-Aldrich (St. Louis, MO, USA). Human IgG was purchased from Jackson Immuno Research Labs (West Grove, PA, USA). NH_2-PEG_{10k}-NH_2 was purchased from Laysan Bio (Arab, AL, USA). Polyethylene glycol-*b*-polylysine (PEG_{5k}-PLL_{33k}) was purchased from Alamanda Polymers (Huntsville, AL, USA). Bis(sulfosuccinimidyl) suberate was purchased from Thermo Fisher Scientific (Waltham, MA, USA). Anti-mouse-CD45RB (clone: MB23G2) was purchased from BioXCell (West Lebanon, NH, USA). Anti-human-CD45 (clone: MEM-28) was purchased from Abcam (Cambridge, United Kingdom). Anti-CD3/CD28 beads were purchased from Thermo Fisher Scientific. All other chemicals and solvents were purchased from Sigma-Aldrich unless otherwise noted. All reagents were used as received unless otherwise noted.

Mice and cell lines. Experiments and handling of mice were conducted under federal, state and local guidelines and with approval from the MIT IACUC. Six- to eight-week-old female Thy1.2$^+$ C57Bl/6 mice, TCR-transgenic Thy1.1$^+$ pmel-1 mice and Nod/SCID/*IL2RG*$^{-/-}$ (NSG) mice were from the Jackson Laboratory. B16F10 melanoma cells and U-87 MG human glioblastoma cells were acquired from the American Type Culture Collection (Manassas, VA, USA) and cultured in Dulbecco's modified Eagle's medium (DMEM). The construct expressing Click beetle red luciferase (CBR-luc) was introduced into U-87 MG cells by lentiviral transduction, for bioluminescence imaging.

Isolation of naive and primed mouse T cells. Spleens from C57Bl/6 or pmel-1 Thy1.1$^+$ mice were ground through a 70-μm cell strainer, and red blood cells were removed by incubation with ACK lysis buffer (2 ml per spleen) for 5 min at 25 °C. Naive CD4$^+$ or CD8$^+$ T cells were isolated from splenocytes directly via magnetic negative selection using an EasySep Mouse CD4$^+$ or CD8$^+$ T cell Enrichment Kit (Stemcell Technologies, Vancouver, Canada), respectively. For activated CD8$^+$ T cells, the splenocytes were washed with PBS and then cultured in RPMI 1640 medium containing 10% FCS, concanavalin A (con-A) (2 μg/ml) and IL-7 (1 ng/ml) at 37 °C for activation. After a 2-d incubation period, dead cells were removed by Ficoll-Pague Plus gradient separation, and CD8$^+$ T cells were isolated by using an EasySep Mouse CD8$^+$ T cell Enrichment Kit. Purified CD8$^+$ T cells were resuspended at 1.5×10^6 cells per ml in RPMI medium containing 10 ng/ml recombinant mouse IL-2. After 24 h, cells were washed three times in PBS and resuspended in buffer or medium for *in vitro* and *in vivo* studies. Con-A-primed mouse CD8$^+$ T cells were used as activated T cells for all of the *in vitro* and *in vivo* studies unless otherwise stated. In a tumor therapy study (**Supplementary Fig. 16**), splenocytes from pmel-1 mice were isolated as described above and cultured in the presence of 1 μM human $gp100_{25–33}$ and culture medium containing mouse IL-2 (10 ng/ml) and IL-7 (1 ng/ml) for 3 d followed by Ficoll-Pague Plus gradient separation. After culture in the medium containing mouse IL-7 (10 ng/ml) for one more day, the pmel-1 CD8$^+$ T cells (>95%) were used for ACT.

Isolation of naive and primed human CD8$^+$ T cells. Total peripheral blood mononuclear cells (PBMCs) were anonymous samples obtained from healthy donors (New York Blood Center, Long Island City, NY, USA). Naive CD8$^+$ T cells were isolated directly by using RosetteSep Human CD8$^+$ T cell Enrichment Cocktail (Stemcell). The human CD8$^+$ T cells were activated in non-tissue-culture plates coated with anti-human-CD3 (2.5 μg/ml) and anti-human-CD28 (1.0 μg/ml) in the presence of human IL-2 (50 UI/ml) for 2 d. Cells were washed three times in PBS and resuspended in buffer or medium for *in vitro* studies.

Measurement of T cell surface reduction activity using the WST-1 assay. T cell surface reduction activity was determined by using a commercial WST-1 assay kit containing WST-1 and an electron coupling reagent (Roche, Basel, Switzerland). Naive or con-A-primed CD8$^+$ T cells from C57Bl/6 mice were suspended in Hank's balanced salt solution (HBSS) at 1×10^6 cells per ml. The commercial WST-1 reagent mixture (10 μl) was added to the T cell suspension (200 μl). The cells were incubated at 37 °C for 1 h. WST-1 formazan production rate was measured with a plate reader (Tecan Infinite M1000 PRO, Tecan, Männedorf, Switzerland) for increased absorbance at 450 nm during the incubation. For the measurement of cell surface reduction in response to TCR triggering, naive or con-A-activated CD8$^+$ T cells were incubated with anti-CD3/CD28 beads (1:1 cell:bead ratio) or gp100 peptide (10 μg/ml) in the presence in IL-7 (1 ng/ml) at 37 °C for 24 h. Cells were washed and resuspended in HBSS (1×10^6 cells/ml) and measured for surface reduction with the same commercial WST-1 reagent mixture after a 1-h incubation at 37 °C.

Synthesis of the NHS-SS-NHS cross-linker. As shown in **Supplementary Scheme 1**, in a 125-ml round-bottom flask, 2-hydroxyethyl disulphide (1.54 g, 10 mmol) was dissolved in tetrahydrofuran (THF, 30 ml, anhydrous) and added dropwise to the solution of phosgene (15 ml, 15 wt. % in toluene, 22 mmol). The mixture was stirred at 25 °C for 10 h followed by the removal of the solvent under vacuum. *N*-hydroxysuccinimide (NHS) (2.3 g, 22 mmol) was dissolved in THF (30 ml, anhydrous) and added as one portion, and then dry triethylamine (1.57 ml, 11 mmol) was injected. The reaction was performed at 40 °C for 16 h. The solvent was removed under vacuum, and the mixture was filtered to remove precipitates. The crude product was purified by silica gel column chromatography (dichloromethane:methanol, 10:1) and recrystallized with icy hexane (80 ml). The resulting white solid was dried under vacuum (3.1 g, yield 71%). ^{1}H-NMR ($CDCl_3$, 500 MHz): δ (ppm)4.58 (*t*, 4H), 3.05 (*t*, 4H), 2.84 (s, 8H). ^{13}C-NMR ($CDCl_3$, 500 MHz): δ 168.77, 151.66, 68.84, 36.68, 25.69. ESI (*m/z*): calcd for $C_{14}H_{16}N_2O_{10}S_2$, 436.4 [M]; found, 459.0 [M+Na]$^+$.

Synthesis of nanogels. NHS-SS-NHS (93.5 μg, 0.214 μmol) dissolved in 9.35 μl DMSO was added to a IL-15-Sa (1,320 μg, 0.0143 μmol) solution in 132 μl PBS pH 7.4. The mixture was rotated at 25 °C for 30 min followed by the addition of 1,188 μl PBS buffer. For NGs that incorporated the CD45-targeting antibody, anti-CD45 (215 μg, 0.0014 μmol) in 31.7 μl PBS buffer was then added to the diluted solution. The reaction mixture was rotated at 25 °C for another 30 min. The preparation of IL-15Sa-NGs without anti-CD45 was similar except that anti-CD45 was replaced with NH_2-PEG_{10k}-NH_2 (715 μg, 0.0715 μmol) in 35.8 μl PBS buffer. Other protein NGs (IL-2Fc-NG, BSA-NG, IgG-NG) were prepared with similar protein concentrations and the same cross-linker/protein mole ratio. The resultant NGs were then washed with PBS (1.5 ml × 3) in an Amicon centrifugal filter (molecular weight cut-off = 100 kDa; Millipore, Billerica, MA, USA). Non-degradable NGs (for example, aCD45/IL-15Sa-NG (non-deg.)) were prepared by using a permanent linker, bis(sulfosuccinimidyl) suberate in lieu of NHS-SS-NHS. To enhance conjugation of aCD45/IL-15Sa-NGs to T cells, before T cell coupling freshly prepared aCD45/IL-15Sa-NG solution was diluted to 1 μg/μl followed by the addition of polyethylene glycol-*b*-polylysine (PEG_{5k}-PLL_{33k}) (43.6 μg, 0.0011 μmol) in 43.6-μl PBS. The mixture was rotated at 25 °C for 30 min and used without further purification.

Fluorescence and biotin labeling of NGs. To prepare fluorescently labeled NGs, cytokine cargos were fluorescently labeled with Alexa Fluor 647 NHS ester (Thermo Fisher Scientific) and purified with Amicon ultracentrifugal filters (molecular weight cut-off 50 kDa). Fluorescent cytokine was mixed with nonlabeled cytokine (10 mol% labeled cytokine) for the preparation of fluorescent NGs following the same procedure as described above. For the preparation of biotinylated NGs, NHS-SS-NHS (93.5 μg, 0.214 μmol) dissolved in 9.35 μl DMSO was added to IL-15Sa (1,320 μg, 0.0143 μmol) solution in 132 μl PBS buffer. The mixture was rotated at 25 °C for 20 min followed by the addition of EZ-Link NHS-LC-LC-biotin (40.6 μg, 0.072 μmol, Thermo Fisher Scientific) in 7.5 μl DMSO. The mixture was rotated at 25 °C for another 20 min and then diluted with 1,188 μl PBS buffer followed by the addition of anti-CD45 (215 μg, 0.0014 μmol) in 31.7 μl PBS buffer. The rest of the procedure was the same as described above.

Characterizations of nanogels. NG formation and complete reaction of protein cargos was verified by HPLC with a size-exclusion column (BioSep-SEC-s4000, Phenomenex, Torrance, CA, USA). NG sizes were determined by transmission electron microscopy (FEI Tecnai, Hillsboro, OR, USA) and dynamic light scattering. NGs were dispersed in deionized water to

a concentration of 0.5 mg/ml. The hydrodynamic size and zeta potential were measured with a Malvern Zetasizer (Malvern, United Kingdom). The final concentrations of NGs were determined with a NanoDrop 1000 Spectrophotometer (Thermo Fisher Scientific).

Release kinetics of cytokines from nanogels. The NGs were dispersed in PBS (0.1 mg/ml) with or without glutathione (GSH, 1 mM) and incubated at 4 °C. At selected time intervals, replicates of solution were analyzed with HPLC equipped with a size-exclusion column to determine the percentage of released cytokine. Released cytokine was also subjected to a MicroFlex matrix-absorption laser desorption instrument time-of-flight instrument (MALDI-TOF, Bruker, Billerica, MA, USA) to determine the molecular weight.

Coupling of nanogels to T cells. In a typical experiment, aCD45/IL-15Sa-NG (950 µg, 0.010 µmol) labeled with Alexa Fluor 647 in 950 µl PBS was added to mouse $CD8^+$ T cells (95×10^6) in 475 µl HBSS followed by incubation at 37 °C for 1 h. The T cells with surface-coupled NGs were collected by centrifugation at 800*g* for 5 min, washed with PBS (1.0 ml × 2) and resuspended in buffer or medium at the desired concentrations for *in vitro* or *in vivo* studies. For measurements of total NG coupling, fluorescently labeled NGs were coupled to T cells, and supernatants were collected and measured for fluorescence intensity at excitation and emission wavelengths of 640 nm and 680 nm, respectively, using a plate reader (Tecan Infinite M1000 PRO). Fluorescence readings were converted to NG concentrations using standard curves prepared from serial dilutions of NG stock solutions. The amount of coupled NG was calculated by subtracting the unbound NG from the total added amount. NG loading per cell was controlled by varying the mass of NGs added to cells for coupling. For the conjugation of NGs lacking anti-CD45 to T cells, IL-15Sa-NG (950 µg, 0.010 µmol) in PBS (950 µl) was first activated with sulfosuccinimidyl 4-(*N*-maleimidomethyl)cyclohexane-1-carboxylate (218 µg, 0.50 µmol) or bis(sulfosuccinimidyl) suberate (286 µg, 0.50 µmol), collected with Amicon ultra-centrifugal filters (molecular weight cut-off 50 kDa) and washed with PBS (1.5 ml × 3), and then added to $CD8^+$ T cells (95×10^6) in 475 µl HBSS followed by incubation at 37 °C for 1 h. Cells were washed and collected similarly. The amount of conjugated NG was determined similarly as described above. Coupling of NGs with or without anti-human-CD45 to human $CD8^+$ T cells followed the procedures described above.

Release kinetics of proteins from NG coupled on T cell surface. Human-IgG-Human IgG-NG labeled with Alexa Fluor 647 fluorescence dye was prepared and coupled to primed polyclonal C57Bl/6 $CD8^+$ T cells as described above. T cells were incubated in medium at 37 °C with or without anti-CD3/CD28 beads at a 1:1 bead:T cell ratio. Cell were collected at selected time points and analyzed by flow cytometry for measurement of mean fluorescence intensity (MFI) over time.

Preparation of liposomes with surface-conjugated antibodies and/or cytokines. Vacuum-dried lipid films composed of 1,2-distearoyl-*sn*-glycero-3-phospho ethanolamine-*N*-[maleimide(polyethylene glycol)-2000 (maleimide-PEG_{2000}-DSPE), cholesterol, hydrogenated soy L-α-phosphatidylcholine (HSPC) and 1,2-distearoyl-*sn*-glycero-3-phosphoethanolamine-*N*-[biotinyl(polyethylene glycol)-2000 (biotin-PEG_{2000}-DSPE) (Avanti Polar Lipids, Alabaster, AL, USA) in a molar ratio of 2.5:27:68:1.5 together with 1% of a fluorescent lipophilic tracer dye DiD were rehydrated in 250 µl of 50 mM 4-(2-hydroxyethyl)-1-piperazineethanesulfonic acid (HEPES) in a 150 mM NaCl buffer (pH 6.5). Lipids were mixed by vortexing every 10 min for 1 h at 62 °C to form vesicles and size-extruded through a polycarbonate membrane (0.2 µm). After washing in excess PBS and spinning down by ultracentrifugation at 110,000*g* for 4 h, liposomes were resuspended in 100 µl PBS per 1.4 mg of lipids. For coupling to the maleimide groups of the liposomes, antibody, cytokine, and antibody and cytokine mixtures at different molar ratios (2–5 mg/ml) were treated with 1.8 mM dithiothreitol (DTT) in the presence of 10 mM EDTA at 25 °C for 20 min to expose free thiols in the hinge region. DTT was subsequently removed by using Zeba desalting columns before mixing with maleimide-bearing liposomes (1:1 wt./wt. for protein:lipid) in PBS. After incubation for 18 h at 25 °C on a rotator, the excess protein was removed by ultracentrifugation using an excess of PBS.

Internalization kinetics of liposomes and nanogels by T cells. Antibody-conjugated liposomes (0.7 mg lipids) in 100 µl PBS were incubated with 20×10^6 primed pmel-1 $Thy1.1^+$ $CD8^+$ T cells in 0.5 ml complete RPMI medium supplemented with 10% FCS for 30 min at 37 °C with gentle agitation every 15 min. Conjugated T cells were washed with PBS (20 ml × 2) to remove unbound liposomes and incubated in RPMI medium with recombinant IL-7 (1.5 ng/ml) and 10% FCS at 0.5×10^6 cells/ml at 37 °C. T cells with surface-coupled biotin-labeled NGs were prepared as described above and suspended in RPMI medium with 10% FCS at 5.0×10^5 cells/ml at 37 °C. At staggered time points, replicates of cells were collected, washed with PBS buffer and then stained with a streptavidin-PE-Cy7 (eBioscience) conjugate to detect surface-localized liposomes or NGs followed by flow cytometry analysis (FACS Canto, BD Biosciences, Franklin Lakes, NJ). Similar assays were performed with anti-CD3- and anti-CD28-activated human $CD8^+$ T cells isolated from human PBMCs. For confocal imaging studies, T cells with surface-coupled Alexa Fluor 647–labeled NGs were collected at different time points, washed with PBS and imaged in chamber slides using an LSM500 laser scanning confocal microscope (Carl Zeiss, Oberkochen, Germany).

***In vitro* proliferation assay of T cells.** Naive pmel-1 $CD8^+$ T cells were labeled with carboxyfluorescein succinimidyl ester (CFSE) and then conjugated with aCD45/IL-15Sa-NG, IL-15Sa-NG, or aCD45/IL-15Sa-NG (non-deg.), respectively, as described above. After removing unbound NGs, T cells were resuspended in RPMI medium with 10% FCS (5.0×10^5 cells/ml) and added to anti-CD3/CD28 beads at a 1:2 bead:T cell ratio. Free IL-15Sa was added to the cells in control groups at an equivalent dose (pulsed or continuous). For the T cells pulsed with free IL-15Sa, cell medium was replaced after a 1-h incubation to wash out the free IL-15Sa. For all of the groups, cell medium was replaced every 3 d, and free IL-15Sa was replenished in the continuous treatment group. At selected time points, replicates of T cells were added with counting beads and washed with flow cytometry buffer (PBS with 2% FCS) followed by aqua live/dead staining. Cells were stained for surface markers (CD8, CD122) with antibodies followed by fixation and permeabilization with Intracellular Fixation & Permeabilization Buffer Set (eBioscience). Cells were then stained intracellularly for phosphorylated STAT5 and Ki67 and analyzed with a flow cytometer (BD Canto, BD Biosciences).

***In vivo* therapy study and T cell expansion.** B16F10 melanoma cells (5.0×10^5) were administered by s.c. injection in the flanks of C57Bl/6 mice on day 0. Mice were sublethally lymphodepleted by total body irradiation (5 Gy) 6 d after tumor cell inoculation. Primed pmel-1 $CD8^+$ T cells (1.0×10^7) alone or with surface-coupled NGs in 200 µl PBS were administered by i.v. injection at day 7. In other groups, free IL-15Sa was administered by i.v. injection immediately after ACT at equivalent total doses (single or multiple doses as indicated). Tumor area (product of two measured orthogonal diameters) and body weight were measured every 2 d. Mice were euthanized when the body weight loss was >20% of the pre-dosing weight, the tumor area reached 150 mm^2 (as a pre-determined end point) or the animal had become moribund.

To monitor *in vivo* T cell expansion and function, mice were euthanized on day 14 for necropsy and flow cytometry analyses. Inguinal lymph nodes (distal or TDLN) and spleen were ground through a 70-µm cell strainer. Splenocytes were then lysed with ACK lysis buffer (2 ml per spleen) for 5 min at 25 °C to remove red blood cells. Blood samples (200 µl) were lysed with ACK lysis buffer (1 ml × 2) for 5 min at 25 °C. Tumors were weighed and ground through a 70-µm cell strainer. All cells were added with counting beads and washed with flow cytometry buffer (PBS with 2% FCS) followed by aqua live/dead staining. Cells were stained for surface markers (CD8, Thy1.1, CD4, NK1.1) with antibodies followed by fixation and permeabilization with Cytofix/Cytoperm (BD Biosciences). Cells were then stained intracellularly for Ki67. After washing with FACS buffer, cells were resuspended in FACS buffer and analyzed by flow cytometry. For intracellular cytokine staining, samples in single-cell suspensions were incubated with gp100 peptide (10 µg/ml) at 37 °C for 2 h followed by the addition of brefeldin A (eBioscience, San Diego, CA, USA) and incubation for another 4 h. Following surface staining as described above, samples were fixed and permeabilized in the same manner and stained with antibodies against interferon (IFN)-γ, tumor necrosis factor (TNF)-α and IL-2. Flow cytometric analysis was performed with a BD Fortessa

doi:10.1038/nbt.4181

instrument (BD Biosciences), and data analysis was performed using FlowJo software (Tree Star, Oregon, USA).

Measurement of serum cytokine levels and liver enzymes for toxicity study. Serum samples from treated mice as described above were collected at day 17 or when the mice were euthanized due to toxicity, and these were then analyzed for cytokine levels using the Cytometric Bead Array (CBA) Mouse Inflammation Kit (BD Biosciences). Serum samples were also sent to IDEXX Reference Laboratories for analysis of alanine transaminase (ALT) and aspartate transaminase (AST).

Measurement of serum antibody. Serum samples were collected from treated mice in different groups at 30 d after ACT. Serum concentration of anti-IL-15Sa was measured by a standard ELISA procedure with calibration of a human-IL-15-specific monoclonal antibody (eBioscience).

Preparation of CAR-T cells for ACT. The huEGFRscFv-BBz chimeric antigen receptor was designed based on the heavy and light chains of cetuximab to form a single-chain variable fragment, which was fused to a portion of the extracellular and transmembrane domains of human CD8α, followed by the intracellular domains of 4-1BB and CD3ζ. The bicistronic vector also encoded truncated human CD19 as a selectable marker, which was placed following a T2A ribosomal skip sequence. The plasmid coding hu EGFRscFv-BBz-CAR was synthesized, and lentivirus packaging was produced by VectorBuilder. Isolated T cells were derived from purchased leukapheresis products obtained from de-identified healthy donors under an IRB-approved protocol. T cells were stimulated with Dynabeads Human T Activator CD3/CD28 (Life Technologies) at a bead:cell ratio of 3:1. T cells were cultured in RPMI 1640 medium supplemented with 10% FBS, HEPES buffer (20 mM), penicillin and streptomycin (1%) and IL-2 (20 IU/ml). T cells were transduced (TDN) with CAR lentivirus and or left untransduced (UTD) 1 d following bead stimulation, and then T cells were expanded for 10 d and cryopreserved until used. Surface expression of the CAR was confirmed and quantified with biotinylated human EGFR protein (ACRO Biosystems).

Cytotoxicity assays of human CAR-T cells. The ability of EGFR-specific CAR-T cells to kill targets was tested in a 20-h luciferase-based killing assay. Transduced T cells and UTD T cells were thawed and rested for 24 h at 37 °C in a 6-well plate in T cell medium. The effectors and targets were mixed together at the indicated effector:target (E:T) ratios and cultured in black-walled 96-well flat-bottom plates with 3×10^4 target cells in a total volume of 200 µl per well in T cell medium. Target cells alone were seeded at the same cell density to determine the maximal luciferase expression (relative light units; RLU_{max}). After 20 h, 100 µl of supernatant per well was removed, and 100 µl of luciferase substrate (Bright-Glo, Promega) was added to the remaining supernatant and cells. Emitted light was measured after 10 min of incubation using the BioTek (SYNERGY NEO2) plate reader. Lysis was determined as $(1 - (RLU_{sample})/(RLU_{max})) \times 100$. Two replicate experiments were performed; each was done in duplicate.

***In vivo* therapy study using human CAR-T cells.** Luciferase-expressing U-87 MG human glioblastoma cells (1.0×10^6) were injected s.c. into NSG mice on day 0 (Jackson Laboratory). Animals received, by i.v. injection, adoptive transfer of activated CAR-T cells (1.0×10^6) alone or with surface-coupled NGs on day 7. In other groups, free IL-15Sa was administered by i.v. injection immediately after ACT at equivalent doses. Tumor area (product of two measured orthogonal diameters) and body weight were measured every 2 d. Mice were also imaged for bioluminescence every week to monitor tumor growth. Mice were euthanized when the body weight loss was >20% of the pre-dosing weight, the tumor area reached 150 mm^2 (as predetermined endpoint) or the animal had become moribund.

***In vivo* bioluminescence imaging.** D-luciferin (PerkinElmer, Waltham, MA, USA) suspended in PBS (15 mg/ml) was injected (150 mg/kg) i.p. 5 min before acquisitions. Bioluminescence images were collected on a Xenogen IVIS Spectrum Imaging System (Xenogen, Alameda, CA, USA). Living Image software Version 3.0 (Xenogen) was used to acquire and quantify the bioluminescence imaging data sets.

Statistical analyses. Statistical analyses were performed using GraphPad Prism software. All values and error bars are mean ± s.e.m., except where indicated differently. Comparisons of tumor growth over time were performed by using two-way ANOVA tests, and comparisons of multiple groups at a single time point were performed by using one-way ANOVA and Tukey's tests. Survival data were analyzed using the log-rank test. Further information on experimental design is available in the Nature Research Reporting Summary linked to this article.

Ethics statement. Experiments and handling of mice were conducted under federal, state and local guidelines and with approval from the Massachusetts Institute of Technology IACUC.

Life Sciences Reporting Summary. Further information on experimental design is available in the **Nature Research Reporting Summary**.

Data availability. The authors declare that the data that support the findings of this study are available from the corresponding author upon request.

49. Han, K.P. *et al.* IL-15:IL-15 receptor–α superagonist complex: high-level co-expression in recombinant mammalian cells, purification and characterization. *Cytokine* **56**, 804–810 (2011).
50. Zheng, Y. *et al. In vivo* targeting of adoptively transferred T cells with antibody- and cytokine-conjugated liposomes. *J. Control. Release* **172**, 426–435 (2013).